

A Nanoring–Nanosphere Molecule, $\{\text{Mo}_{214}\text{V}_{30}\}$: Pushing the Boundaries of Controllable Inorganic Structural Organization at the Molecular Level

Bogdan Botar,[†] Paul Kögerler,[‡] and Craig L. Hill^{*†}

Department of Chemistry, Emory University, Atlanta, Georgia 30322, and Ames Laboratory, Iowa State University, Ames, Iowa 50011

Received February 6, 2006; E-mail: chill@emory.edu

The self-assembly of hierarchical inorganic structures and the control of their formation is fundamental in biological systems and useful in synthetic ones. Biomineralization processes,¹ the deliberate formation of functional nanostructures,² and the generation of crystals with multiple structural domains are just a few examples. These processes pertain directly to controlled functionalization of nanosized metal–oxo cluster frameworks.

A. Müller and co-workers have pioneered routes to giant polymolybdates of two predominant structural types: cyclic, or ring-shaped structures (exemplified by $\{\text{Mo}_{154}\}$, $\{\text{Mo}_{176}\}$, $\{\text{Mo}_{128}\text{Eu}_4\}_2$)³ and hollow, spherical structures (keplerates; exemplified by $\{\text{Mo}_{102}\}$,^{4a} $\{\text{Mo}_{132}\}$,^{4b} $\{\text{Mo}_{72}\text{V}_{30}\}$,^{4c,d} and $\{\text{Mo}_{72}\text{Fe}_{30}\}$ ^{4e}). Both the rings and spheres are constituted by transferable fragments (“building blocks”) that assemble under symmetry constraints.³ Given the extraordinary structural complexity yet extensive alterability of these clusters, particularly of molybdenum-blue species (in which a large number of Mo(4d) electrons are delocalized within well-defined structural compartments),⁵ we have endeavored to determine whether these nanometer-sized species can be orchestrated into even larger assemblies with a commensurately more complex degree of molecular organization. Beyond the immediate relevance to supramolecular chemistry, incorporation of magnetic centers into these large structures can lead to extended spin topologies for which unusual magnetic phenomena are observed.⁶ In addition, these partially reduced and highly magnetic species could play significant roles in applications such as molecular electronics⁷ and the imaging of biological tissues.⁸ We report here how a carefully controlled polymerization–reduction process can lead to a single mesoscopic molecule containing the two basic types of nano-architectures noted above.

Acidification of a mixture of vanadate and molybdate followed by controlled reduction with hydrazine sulfate and subsequent addition of KCl (details are given in the Supporting Information, SI) leads to a vanadium(IV)-containing nanoring–nanosphere assembly, $\text{K}_{43}\text{Na}_{11}(\text{VO})_4[\{\text{Mo}^{\text{VI}}_{72}\text{V}^{\text{IV}}_{30}\text{O}_{282}(\text{H}_2\text{O})_{66}(\text{SO}_4)_{12}\}\{\text{Mo}^{\text{VI}}_{114}\text{Mo}^{\text{V}}_{28}\text{O}_{432}(\text{OH})_{14}(\text{H}_2\text{O})_{58}\}] \cdot \text{ca. } 500 \text{ H}_2\text{O} = \{\text{Mo}_{214}\text{V}_{30}\}$ (**1**). Raman spectra (Figure S1 in the SI) and kinetic precipitation using K^+ , both as a function of time, reveal that **1** derives from initial formation of the keplerate-type cluster $\{\text{Mo}_{72}\text{V}_{30}\}$,⁹ followed by subsequent slower (16–24 h using the given synthetic conditions) formation and attachment of molybdenum-blue, ring-type species which display a very characteristic line-pattern in the 200–900 cm^{-1} region.⁵ Once the nanoring units are generated, **1** is easily precipitated by addition of KCl. Evidence for the initial formation of keplerate followed by a slower ring attachment process is also supported by the fact that using conditions favoring initial ring formation (e.g. lower pH and/or using a larger amount of reducing agent) fails to produce **1** regardless of the reaction time. Instead,

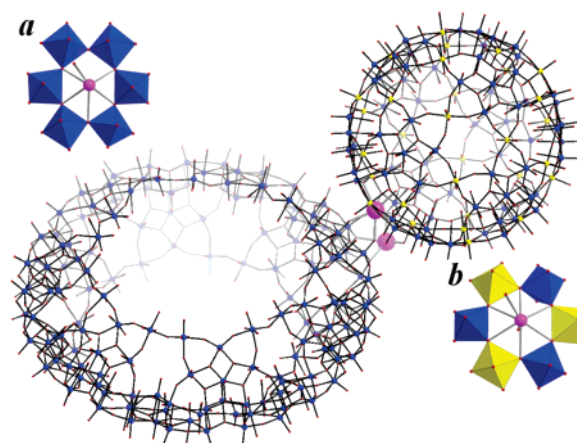


Figure 1. Ball-and-stick representation of the ring-sphere anion in **1** (Mo: blue, O: red, V: yellow, K: purple). Apart from the two K^+ sites shown connecting the $\{\text{Mo}_{142}\}$ ring and the $\{\text{Mo}_{72}\text{V}_{30}\}$ sphere, additional K^+ cations bind to $\{\text{Mo}_6\text{O}_6\}$ pores present in the ring substructure (a) and to $\{\text{Mo}_3\text{V}_3\text{O}_6\}$ pores of the spherical substructure (b).

only ring-type species (i.e., of the $\{\text{Mo}_{154}\}$ - or $\{\text{Mo}_{176}\}$ -type) can be isolated from such mixtures.

A structural investigation (all details in the SI) of **1** reveals an open “clam-like” nanoscopic assembly (ca. 6 nm in length) comprising a spherical $\{\text{Mo}^{\text{VI}}_{72}\text{V}^{\text{IV}}_{30}\}$ anion and a ring-shaped $\{\text{Mo}_{142}\}$ anion linked by two K centers acting as a hinge (Figure 1). Interestingly, the spherical subunit present in **1** exhibits a regular icosahedral structure (virtual I_h symmetry) in contrast to the recently reported more distorted D_{5d} $\{\text{Mo}_{72}\text{V}_{30}\}$ cluster,^{4c,d} with potential implications for the magnetic properties (see below). The lower symmetry of the discrete $\{\text{Mo}_{72}\text{V}_{30}\}$ cluster is due to the presence of two parallel $\{\text{KSO}_4\}_5$ rings which coordinate from the inside to the cluster shell resulting in the flattening of the sphere at two opposite ends. In **1**, these internal rings are missing, and the spherical cluster shell contains only 12 disordered tridentate sulfate ligands. The other subunit of **1** is a $\{\text{Mo}_{142}\}$ cluster-anion that can be viewed as a tetradecameric $\{\text{Mo}_{154}\} = [\{\text{Mo}_2\}\{\text{Mo}_8\}\{\text{Mo}_1\}]_{14}$ -type ring in which ca. 6 out of the 14 loosely bound $\{\text{Mo}_2\} = \{\text{Mo}^{\text{VI}}\text{O}_2(\text{H}_2\text{O})\}_2(\mu\text{-O})^{2+}$ units (two corner-sharing octahedra with three terminal sites) are missing, a common pattern for derivatives of molybdenum-blue, ring-type structures. These vacant sites are delocalized over the 14 possible positions of the ring based on the underoccupancy of every atom of the $\{\text{Mo}_2\}$ -type unit. As previously established, all $\{\text{Mo}_{154}\}$ ring-type clusters contain 28 partially delocalized Mo(4d) electrons (two in each $\{\text{Mo}_5(\mu_3\text{-O})_2\text{O}_4\text{H}\}$ central compartment). Bond valence sum (BVS) values for these Mo centers and the $\mu_3\text{-O}$ atoms in the $\{\text{Mo}_5(\mu_3\text{-O})_2\text{O}_4\text{H}\}$ units of **1** are in good agreement with those previously reported for the $\{\text{Mo}_{154}\}$ -type species, strongly suggesting that these units are identical.⁵

[†] Emory University.

[‡] Iowa State University.

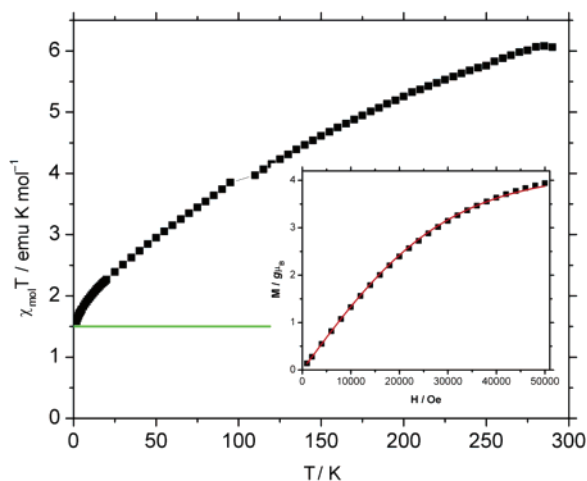


Figure 2. Experimental temperature-dependence of χT for **1** at 0.1 Tesla and 2–290 K (black squares) indicating strong antiferromagnetic coupling between the $S = 1/2$ vanadyl groups within the I_h -symmetric $\{\text{Mo}_{72}\text{V}_{30}\}$ substructure. The horizontal green line marks the background due to four uncoupled vanadyl countercations that are disordered in the crystalline lattice. (Inset) Field-dependence of the magnetization at 2.0 K. The red curve represents the best fit to a scaled spin- $1/2$ Brillouin function ($g = 2.0$), yielding 4.1 uncorrelated $S = 1/2$ centers per molecular unit.

Extended Hückel MO calculations also indicate a nearly identical electron structure, with very similar frontier orbital compositions, especially 14 nearly degenerate highest occupied MOs of predominantly Mo(4d) character mostly localized over the outermost Mo positions. The previously documented affinity of the K^+ cations for the $\{\text{Mo}_3\text{V}_3\text{O}_6\}$ hexagonal pores of the keplerate-type clusters is clearly evident in **1** (all 20 pores of the spherical subunit appear to be capped by K^+ cations although some of these were refined with half occupancy based on their large thermal parameters).^{4c,d,6c} Notably, the ring-type subunit of **1** also contains 14 $\{\text{Mo}_6\text{O}_6\}$ hexagonal pores, some of which are capped by K^+ cations in a similar fashion.¹⁰

The vis-NIR electronic spectrum of **1** (Figure S2) shows three very intense, broad absorption bands in the 400–1200 nm range. The lowest-energy band responsible for the resonance Raman effect ($\lambda_e = 1064$ nm) with a maximum at 1055 nm is the result of homonuclear IVCT (intervalence charge transfer) transitions of the $\text{Mo}^{\text{V}} \rightarrow \text{Mo}^{\text{VI}}$ type, based on the difference in optical electronegativity between the atoms involved.¹¹ The 730-nm band, which is the dominant feature in the spectra of mixed valence $\text{Mo}^{\text{V}}/\text{Mo}^{\text{VI}}$ ring-type species is also the result of $\text{Mo}^{\text{V}} \rightarrow \text{Mo}^{\text{VI}}$ type IVCT. The highest-energy band (maximum at 525 nm) is very likely due $\text{V}^{\text{IV}} \rightarrow \text{Mo}^{\text{VI}}$ heteronuclear IVCT since it is not present in the spectra of molybdenum-only ring-type species but is the prominent feature in the spectrum of the spherical $\{\text{Mo}_{72}\text{V}_{30}\}$ cluster.^{4c,d} The resonance Raman spectrum of **1** in water (Figure S1) is very similar to that of the $\{\text{Mo}_{154}\}$ -type species supporting a similar electron delocalization involving the $\{\text{Mo}_5(\mu_3\text{-O})_2\text{O}_4\text{H}\}$ units.⁵ This is also consistent with only the ring and not the sphere in **1** being partially reduced.

The magnetic properties of **1** are indicative of the strong antiferromagnetic coupling of the $30 S = 1/2 \text{VO}^{2+}$ groups within the $\{\text{Mo}_{72}\text{V}_{30}\}$ entity defining the corners of an icosidodecahedron and the presence of four uncoupled vanadyl cations in the crystal lattice (Figure 2). Once the contribution of the uncorrelated spin centers is subtracted, the resulting temperature dependence of χ (which does not exhibit Curie–Weiss law behavior) nearly matches that of the isolated $\{\text{Mo}_{72}\text{V}_{30}\}$ cluster: χT rapidly rises with increasing temperature for both compounds despite the large

effective nearest-neighbor exchange energy of $J/k_B \approx -220$ K (mediated by $-\text{O}-\text{Mo}^{\text{VI}}-\text{O}-$ pathways). The rapid onset of χT even at lowest temperatures can only be explained by the presence of low-lying $S > 0$ spin states that can be populated even at such low temperatures. While we initially believed that these states emerge from splitting due to the decreased symmetry (and thus from a spread of different nearest-neighbor V–V interactions) in the discrete $\{\text{Mo}_{72}\text{V}_{30}\}$ cluster, the results for **1** imply that the next-nearest neighbor coupling J' , likely two orders of magnitude smaller than J , is significant and results in low-lying spin states.

Complex **1** exhibits three levels of controllable structural organization: the multi-Mo “building blocks” including the pentagonal $\{(\text{Mo})\text{Mo}_5\}$ and the $\{\text{Mo}_2\}$ units, the ring and sphere components, and **1**, in which these two nanostructures are joined. The implication is that other and still larger multinanounit assemblies may be possible.

Acknowledgment. The present research is supported by DOE (Grant DOE-FG02-03-ER1546 to C.L.H.). Ames Laboratory is operated for the U.S. Department of Energy by Iowa State University under Contract No. W-7405-Eng-82.

Supporting Information Available: Crystallographic details and CIF file for **1**; synthesis details, TGA-DSC, spectroscopic (IR, Raman, vis-NIR) and magnetic data. This material is available free of charge via the Internet at <http://pubs.acs.org>.

References

- (1) (a) Mann, S.; Webb, J.; Williams, R. J. P. *Biomaterialization: Chemical and Biochemical Perspectives*; VCH Publishers Inc.: New York, 1989. (b) Mann, S.; Ozin, G. A. *Nature* **1996**, *382*, 313. (c) Ozin, G. A. *Acc. Chem. Res.* **1997**, *30*, 17–27. (d) Combs, N.; Khushalani, D.; Oliver, S.; Ozin, G. A.; Shen, G. C.; Sokolov, I.; Yang, H. *J. Chem. Soc., Dalton Trans.* **1997**, 3941–3952.
- (2) (a) Mallouk, T. E. *Science* **2001**, *291*, 443–444. (b) Sanchez, C.; Soller-Illia, G. J. de A. A.; Ribot, F.; Lalot, T.; Mayer, C. R.; Cabuil, V. *Chem. Mater.* **2001**, *13*, 3061–3083.
- (3) (a) Müller, A.; Peters, F.; Pope, M. T.; Gatteschi, D. *Chem. Rev.* **1998**, *98*, 239–271. (b) Müller, A.; Kögerler, P.; Dress, A. W. M. *Coord. Chem. Rev.* **2001**, *222*, 193–218. (c) Müller, A.; Kögerler, P.; Kuhlmann, C. *Chem. Commun.* **1999**, 1347–1358. (d) Cronin, L.; Beugholt, C.; Krickemeyer, E.; Schmidtman, M.; Bögge, H.; Kögerler, P.; Luong, T. K. K.; Müller, A. *Angew. Chem., Int. Ed.* **2002**, *41*, 2805–2808.
- (4) (a) Müller, A.; Shah, S. Q. N.; Bögge, H.; Schmidtman, M.; Kögerler, P.; Hauptfleisch, P.; Leiding, S.; Wittler, K. *Angew. Chem., Int. Ed.* **2000**, *39*, 1614–1616. (b) Müller, A.; Polarz, S.; Das, S. K.; Krickemeyer, E.; Bögge, H.; Schmidtman, M.; Hauptfleisch, B. *Angew. Chem., Int. Ed.* **1999**, *38*, 3241–3245. (c) Botar, B.; Kögerler, P.; Hill, C. L. *Chem. Commun.* **2005**, 3138–3140. (d) Müller, A.; Todea, A. M.; Slageren, J.; Dressel, M.; Bögge, H.; Schmidtman, M.; Luban, M.; Engelhardt, L.; Rusu, M. *Angew. Chem., Int. Ed.* **2005**, *44*, 3857–3861. (e) Müller, A.; Sarkar, S.; Shah, S. Q. N.; Bögge, H.; Schmidtman, M.; Sarkar, Sh.; Kögerler, P.; Hauptfleisch, B.; Trautwein, A. X.; Schünemann, V. *Angew. Chem., Int. Ed.* **1999**, *38*, 3238–3241.
- (5) Müller, A.; Serain, C. *Acc. Chem. Res.* **2000**, *33*, 2–10.
- (6) (a) Müller, A.; Luban, M.; Schröder, C.; Modler, R.; Kögerler, P.; Axenovich, M.; J. Schnack, Canfield, P.; Bud'ko, S.; Harrison, N. *ChemPhysChem* **2001**, *2*, 517–521. (b) Schröder, C.; Nojiri, H.; Schnack, J.; Hage, P.; Luban, M.; Kögerler, P. *Phys. Rev. Lett.* **2005**, *94*, 017205-1–017205-4. (c) Botar, B.; Kögerler, P.; Müller, A.; Garcia-Serres, R.; Hill, C. L. *Chem. Commun.* **2005**, 5621–5623.
- (7) Leuenberger, M. N.; Loss, D. *Nature* **2001**, *410*, 789–793.
- (8) Rodríguez E.; Roig A.; Molins E.; Arús C.; Quintero M. R.; Cabañas M. E.; Cerdán S.; Lopez-Larrubia P.; Sanfeliu C. *NMR Biomed.* **2005**, *18*, 300–307.
- (9) The first part of the synthesis of **1** follows very closely the synthesis of $\{\text{Mo}_{72}\text{V}_{30}\}$ reported in ref 4c.
- (10) Incorporation of K^+ cations into the pores of a ring has been previously observed for a $\{\text{Mo}_{176}\}$ -type cluster where 16 K^+ cations are linked by 16 SO_4 ligands occupying alternate positions: Müller, A.; Toma, L.; Bögge, H.; Schmidtman, M.; Kögerler, P. *Chem. Commun.* **2003**, 2000–2001. In contrast, **1** contains no SO_4 ligands in the ring-subunit.
- (11) So, H.; Pope, M. T. *Inorg. Chem.* **1972**, *11*, 1441–1443.

JA060886S